Supplementary Information

Synthesis of active, robust and cationic Au_{25} cluster catalysts on double metal hydroxide by long-term oxidative aging of $Au_{25}(SR)_{18}$

Shinya Masuda,[†] Shinjiro Takano,[†] Seiji Yamazoe[‡] and Tatsuya Tsukuda[*,†,§]

[†]*Department of Chemistry, Graduate School of Science, The University of Tokyo,*
Hongo 7-3-1, Bunkyo-Ku, Tokyo 113-0033, Japan

[‡]*Department of Chemistry, Graduate School of Science, Tokyo Metropolitan University, 1-1 Minami-Osawa, Hachioji-shi, Tokyo 192-0397, Japan*

[§]*Elements Strategy Initiative for Catalysts and Batteries (ESICB), Kyoto University,*
Katsura, Kyoto 615-8520, Japan

1. Methods

1.1 Chemicals

Hydrogen tetrachloroaurate tetrahydrate ($HAuCl_4{\cdot}4H_2O$) was purchased from Tanaka Precious Metals. All solvents (except THF), silica for column chromatography, sodium borohydride ($NaBH_4$), $Mg(NO_3)_2{\cdot}6H_2O$, $Co(NO_3)_2{\cdot}6H_2O$, $Al(NO_3)_3{\cdot}9H_2O$, $Ce(NO_3)_3{\cdot}6H_2O$, sodium hydroxide ($NaOH$), and sodium carbonate (Na_2CO_3) were purchased from FUJIFILM Wako Pure Chemical Industries. Tetrahydrofuran (dehydrated) and $Ni(NO_3)_2{\cdot}6H_2O$ were purchased from Kanto Chemicals. 2-Phenylethanethiol (PET), captopril (Capt) and trans-2-[3-(4-tert-butylphenyl)-2-methyl-2-propenylidene]malononitrile (DCTB) were purchased from Tokyo Chemical Industry. Tetraoctylammonium bromide (TOAB), 2-(Boc-amino)ethanethiol (BaET), Sephadex® LH-20 (for gel permeation column chromatography), deuterated benzyl alcohol ($C_6H_5CD_2OH$) and boron nitride (BN) were purchased from Sigma-Aldrich. CeO_2 support (JRC-CEO-2) was kindly supplied by the Catalysis Society of Japan. The water used was Milli-Q grade (>18 MΩ).

1.2 Preparation of various double metal hydroxide (DMH) supports

Various DMH supports were prepared by a typical co-precipitation method in basic aqueous solution.[S1] 15 mmol of $M^{2+}(NO_3)_2$ ($M^{2+} = Mg^{2+}$, Ni^{2+}, and Co^{2+}) salt and 5 mmol of $M^{3+}(NO_3)_2$ ($M^{3+} = Al^{3+}$ and Ce^{3+}) salt (ratio of $M^{2+}:M^{3+} = 3:1$) were dissolved in 20 mL of water (solution A). 20 mL of basic aqueous solution containing NaOH and Na_2CO_3 with molar ratio of $CO_3^{2-}/M^{3+} = 2$ and $OH^-/(M^{2+}+M^{3+}) = 1.6$ (solution B) was stirred at 60 °C (around 1000 rpm). Then, solution A was added dropwise (0.5 mL/min) into solution B under stirring. After aging for 12 h at 60 °C without stirring, the sample was washed with water using centrifugation until the pH reached around 7–8. Finally, the slurry was dried at 80 °C for 24 h and the obtained solid was thoroughly grinded for further use.

1.3 Synthesis of $Au_{25}(PET)_{18}^-$ and $Au_{25}(PET)_{18}^0$

PET-protected Au_{25} clusters ($Au_{25}(PET)_{18}$) were synthesized by previously reported procedures with slight modifications.[S2] $HAuCl_4{\cdot}4H_2O$ (2.54 mmol, 1.06 g) and TOAB (2.85 mmol, 1.56 g) were dissolved in 70 mL of THF and stirred for 15 min (the color of the solution turned from yellow to orange). 1.8 mL of PET was added dropwise into the solution and stirred for an additional 3 h to make a clear solution. Then, freshly-prepared ice-cold aqueous $NaBH_4$ solution (25.5 mmol in 24 mL of water) was added at once. The suspension was continuously stirred for 2 days. Then, the THF layer was collected by passing the suspension through a filter and evaporating to obtain crude product. The crude product was added to MeOH solution and washed at least six times using centrifugation. The precipitate was extracted with DCM to remove insoluble Au-thiolate oligomers and evaporated to dryness. Finally, the product was recrystallized in toluene by layering hexane (toluene:hexane = 1:10, concentration: 20 mg/mL in toluene) and collected after 2 days as $Au_{25}(PET)_{18}^-$.

$Au_{25}(PET)_{18}^0$ was prepared by silica-gel column chromatography of the $Au_{25}(PET)_{18}^-$ (hexane:DCM = 2:1 as eluent). After column chromatography, the product was recrystallized in toluene by layering EtOH (toluene:EtOH = 1:10, concentration: 20 mg/mL in toluene) and collected after 2 days.

1.4 Synthesis of $Au_{25}(BaET)_{18}^-$

$Au_{25}(BaET)_{18}^-$ was synthesized by ligand exchange reaction from $Au_{25}(PET)_{18}^-$. 70 mg of $Au_{25}(PET)_{18}^-$ clusters was dissolved in 4 mL of DCM and stirred. 0.712 mL of BaET (25 equiv. to PET) was added dropwise and stirred for 8 h. After stirring, the mixture was evaporated to obtain a crude product which was then precipitated by adding to 90 mL of hexane. After centrifugation (3500 rpm, 0 °C, 30 min), the precipitate was extracted with DCM and evaporated. Again, the clusters were dissolved in 4 mL of DCM and 0.712 mL of BaET was added dropwise under stirring. After 12 h of stirring, the mixture was evaporated and the crude product was precipitated by adding to 90 mL of hexane. After centrifugation (3500 rpm, 0 °C, 30 min), the precipitate was extracted with DCM and evaporated. Finally, the product was purified using gel permeation column chromatography (GPC, Sephadex® LH-20) in the MeOH solution (50.5 mg, yield: 65.9 %). (Note that ligand exchange was conducted twice because even if 50 equiv. of BaET ligand was used, ligand exchange was not completed at once: one or two PET ligands still remained.)

1.5 Synthesis of $Au_{25}(Capt)_{18}^-$

Captopril-protected Au_{25} clusters ($Au_{25}(Capt)_{18}^-$) were synthesized by the previously reported procedure with modifications.[S3] $HAuCl_4 \cdot 4H_2O$ (1.0 mmol, 411.5 mg) and TOAB (1.15 mmol, 628 mg) were dissolved in 40 mL of MeOH and stirred for 20 min (the color of the solution turned from yellow to orange). 20 mL of MeOH solution containing Captopril (5 mmol, 1086 mg) was rapidly added to the above solution. After 30 min of stirring, freshly-prepared ice-cold aqueous $NaBH_4$ solution (10 mmol in 20 mL of water) was added at once and continuously stirred for 48 h. The suspension was centrifuged to remove insoluble impurities, and the supernatant was evaporated. The obtained solid was extracted with a slight amount of MeOH and precipitated in EtOH solution (80 mL). The precipitate was collected by centrifugation and extracted with MeOH solution. The solution was filtered to remove the remaining insoluble impurities, and evaporated. Then, the solid was extracted with a slight amount of MeOH and re-precipitated in EtOH solution (80 mL). This washing process was repeated three times. Finally, the product was purified using GPC in the MeOH solution.

1.6 Loading of $Au_{25}(BaET)_{18}^-$ on various DMH supports or CeO_2

0.5 g of DMH support or CeO_2 was dissolved in 100 mL of toluene and sonicated for 30 min to make a homogeneous suspension. The resulting solution was stirred at 0 °C at least for 30 min to reach equilibrium. $Au_{25}(BaET)_{18}^-$ (8.30 mg, 1 wt% on the basis of gold weight) was dissolved in toluene using a volumetric flask (100 mL) and the UV-vis absorption spectrum of the solution was measured to calculate the accurate amount of cluster loading. The cluster solution was added dropwise into the above solution containing support using a syringe pump (pumping rate: 1 mL/min). After stirring for 30 min at 0 °C, the suspension was filtered with a membrane filter and washed with toluene and hexane. The residue was dried *in vacuo.* and grinded for further use. The filtrate was evaporated and the residue was dissolved in toluene using a volumetric flask (10 mL) for measuring the UV-vis absorption spectrum. The loading amount was estimated from the difference of absorption intensity of the cluster solution at 698 nm before and after loading. The calculated amount of $Au_{25}(BaET)_{18}^-$ was successfully loaded on each DMH support as shown in Fig. S3.

1.7 Loading of $Au_{25}(Capt)_{18}^-$ on Co_3Ce support

Loading of $Au_{25}(Capt)_{18}^-$ on the Co_3Ce support was conducted using a similar procedure as that of $Au_{25}(BaET)_{18}^-$. The only difference was the use of MeOH as solvent instead of toluene. Successful loading of $Au_{25}(Capt)_{18}^-$ was confirmed by UV-vis absorption spectra as shown in Fig. S4.

1.8 Loading of $Au_{25}(PET)_{18}^0$ on Co_3Ce support

Loading of $Au_{25}(PET)_{18}^0$ on the Co_3Ce support was conducted using a similar procedure as that of $Au_{25}(BaET)_{18}^-$. Because $Au_{25}(PET)_{18}^0$ clusters are not adsorbed on the Co_3Ce support, the mixture of clusters and support was evaporated after 30 min of stirring at 0 °C instead of filtration.

1.9 Aging of catalysts

The cluster-supported materials were aged in air or vacuum (<100 Pa) at various temperatures. The heating rate was fixed to 5 °C/min and then the temperature was kept at the desired level for 2–30 h.

1.10 Characterization

Powder X-ray diffraction (PXRD) patterns were recorded at room temperature using a diffractometer and D/teX Ultra 250 detector (SmartLab 3, Rigaku), with Cu Kα characteristic radiation (λ = 1.5405 Å). Measurements were conducted in the 2θ range of 10–80 degrees. SmartLab Studio II (Rigaku) was used for measurement and analysis. Nitrogen adsorption-desorption isotherms were measured at −196 °C using a BELSORP-mini II system (MicrotracBEL Corp.). Samples were degassed at 150 °C for 12 h under vacuum to vaporize the physisorbed water using BEL-PREP-vacII. Specific surface area was calculated by the BET (Brunauer–Emmett–Teller) method using nitrogen adsorption data ranging from p/p_0 = 0.05 to 0.35. The negative-mode ESI-MS spectrum of the product was recorded using a JEOL JMS-T100LC time-of-flight mass spectrometer. Sample solutions were prepared by dissolving the clusters in DCM/CH_3CN (1/1) solution (0.5 mg/mL). The sample solution was directly infused at a flow rate of 3.0 mL/h via a syringe pump. MALDI mass spectrum was recorded using a time-of-flight mass spectrometer (AXIMA-CFR, Shimadzu); DCTB was used as a matrix. The specimen for MALDI-MS was prepared by drop-casting a toluene dispersion of $Au_{25}(PET)_{18}^0$ and DCTB ([$Au_{25}(PET)_{18}^0$]:[DCTB] = 1:200) onto a sample plate. Optical absorption spectra were recorded by using a spectrophotometer (V-670 or V-630, JASCO). Thermogravimetry-differential thermal analysis (TG-DTA) was conducted using a SII TG-DTA 7200 (Hitachi High-Tech Science) instrument. $Au_{25}(BaET)_{18}$ cluster was put in an aluminum pan and heated to 300 °C at a heating rate of 5 °C/min. Co_3Ce support and $Au_{25}(BaET)_{18}/Co_3Ce$ were also put in an aluminum pan and heated to 150 °C at a heating rate of 5 °C/min and kept for 12 h. After that, the samples were heated to 500 °C at a heating rate of 5 °C/min and kept for 1 h. Scanning electron microscopy (SEM) was performed on a FEI Magellan 400L. Aberration-corrected transmission electron microscope (ACTEM) images were collected using a JEM-ARM200F microscope operated at an acceleration voltage of 80 kV, under 1×10^{-5} Pa at 298 K in the specimen column. The ACTEM sample was prepared by dropcasting the EtOH dispersion of the catalysts onto copper grids (SHR-C075, Okenshoji). Aberration-corrected high-angle annular dark field scanning transmission electron microscope (AC-HAADF-STEM) images were collected using a JEM-ARM200F microscope operated at an acceleration voltage of 120 kV, under 1×10^{-5} Pa at 298 K in the specimen column. AC-HAADF-STEM samples were prepared by dropcasting the hexane and MeOH dispersion of $Au_{25}(BaET)_{18}/Co_3Ce$ and $Au_{25}(BaET)_{18}/Co_3Ce$-150-12 catalysts, respectively, onto lacey carbon film coated copper grids (Cu200LC, ALLIANCE Biosystems, Inc.). X-ray photoelectron spectroscopy (XPS) was performed using a PHI 5000 VersaProbe (ULVAC-PHI) instrument with the Al-Kα X-rays (1486.6 eV) at an energy resolution of 0.2 eV. The sample pellets were mounted on carbon tape for the measurement. Calibration of energy was conducted by combining the Au $4f_{7/2}$ of Au foil and C 1s of carbon tape. Firstly, the peak of Au $4f_{7/2}$ of Au foil was adjusted to 84.0 eV and the energy shift was applied to C 1s as well. The C 1s of the Au_{25}/Co_3Ce sample was adjusted to the same value as that of Au foil and the energy shift was applied to the Au 4f spectrum. Au L_3-edge X-ray absorption spectroscopy (XAS) was conducted in the fluorescence mode using an ion chamber for the I_0 and 19 solid state detector (SSD) for I_1 detector in the BL01B1 beamline at SPring-8 of the Japan Synchrotron Radiation Research Institute (proposal number: 2020A0672 and 2021A1200). The incident X-ray beam was monochromatized by a Si (111) double-crystal monochromator. X-ray energy was calibrated using Au foil for Au L_3-edge. XAFS data were analyzed by software (xTunes).[S4] The k^3-weighted χ spectra in the k range of 3–14 $Å^{-1}$ were Fourier-transformed into the r space. The curve-fitting analysis was conducted over the r range of 1.4–3.1 Å.

1.11 Catalytic oxidation of benzyl alcohol

Catalytic oxidation of benzyl alcohol was conducted by controlling the temperature using *Chemistation* equipment (PPS-1510 and PPS-2510, EYELA). As for the conditions in Table 1, the tube was charged with 10 mg of samples, biphenyl (102 μmol) as internal standard and stirrer bar, and then 1 mL toluene solution containing benzyl alcohol (102 mM) was added into the tube, followed by stirring at 80 °C. The gas phase was immediately replaced with pure O_2 using a balloon. After 1 h, the solution was immediately put in an ice bath and the catalyst was separated using a syringe filter to quench the reaction. The substrate and products were analyzed by gas chromatograph (GC, GC-2025, Shimadzu) with a flame ionization detector.

As for the conditions in Table 2, the tube was charged with 5 or 15 mg of samples together with stirrer bar, and 1 mL or 15 mL of aqueous benzyl alcohol solution (51 mM) was added into the tube in the case of Au 0.5 mol% or Au 0.1 mol%, respectively. The tube was immediately stirred at 30 °C and the gas phase was replaced with pure O_2 using a balloon. 21.05 mg of K_2CO_3 (300 mol% to substrate) was initially added into the tube, while 50 μL or 750 μL of aqueous NaOH or KOH solution (3.05 mM) was added just before the replacement of gas. After 30 min, an excess amount of HCl (35%, 200 μL) was added to quench the reaction. The substrate and products were extracted with toluene (1–2 mL) four times. Excess NaCl was added to the solution to increase the extraction efficiency. The extract was dried over $MgSO_4$ and diluted to 10 mL using a volumetric flask to adjust the concentration. Obtained extracts were analyzed by the aforementioned GC. To investigate the time-course reactivity, 1 mL of aliquot was sampled at the given time and extracted by the same procedure in the case of Au 0.1 mol%.

1.12 Recycling test of Au_{25}/Co_3Ce catalyst in benzyl alcohol oxidation

A test tube was charged with 5 mg of samples together with stirrer bar, and 1 mL of aqueous benzyl alcohol solution (51 mM) was added into the tube. The tube was immediately stirred at 30 °C and 50 μL of aqueous KOH solution (3.05 mM) was added, then the gas phase was replaced with pure O_2 using a balloon. After 30 min, the suspension was immediately centrifuged (14000 rpm, 1 min) and the supernatant was quenched with an excess amount of HCl (35%, 200 μL). The residue was washed twice with 1 mL of water and the supernatant was also collected for extraction. Finally, the residue was immediately dissolved in the new reaction solution and used for the next reaction by adding KOH and replacing the gas. After the second cycle, the same procedure was used to wash the catalyst and to collect the reaction product and used for the next reaction. After the reaction, the catalyst was washed twice and the supernatant was quenched. The substrate and products were extracted with toluene (2 mL) four times. Excess NaCl was added to the solution to increase the extraction efficiency. The extract was dried over $MgSO_4$ and diluted to 10 mL using a volumetric flask to adjust the concentration. The obtained extract was analyzed by GC (GC-2025, Shimadzu) with a flame ionization detector.

2. Results

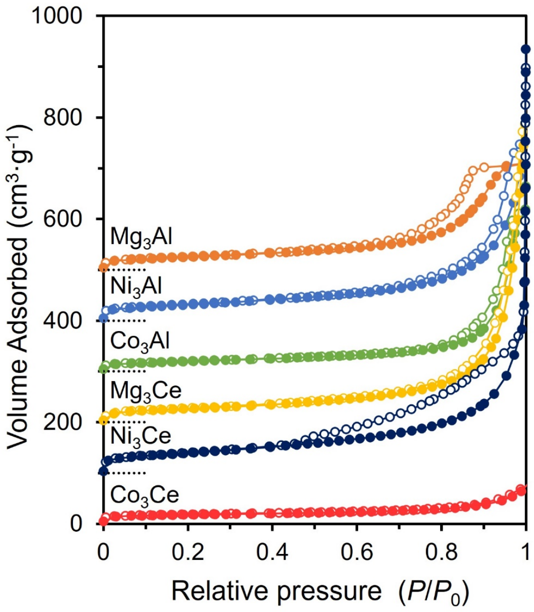

Fig. S1 N_2 adsorption desorption isotherm of various DMH supports.

Table S1 Specific surface area and pore volume of various DMH supports calculated by BET method

DMH support	specific surface area ($m^2 \cdot g^{-1}$)	pore volume ($cm^3 \cdot g^{-1}$)
Mg_3Al	89.9	0.32
Ni_3Al	112	0.47
Co_3Al	68.9	0.46
Mg_3Ce	93.8	0.77
Ni_3Ce	140	0.42
Co_3Ce	58.5	0.084

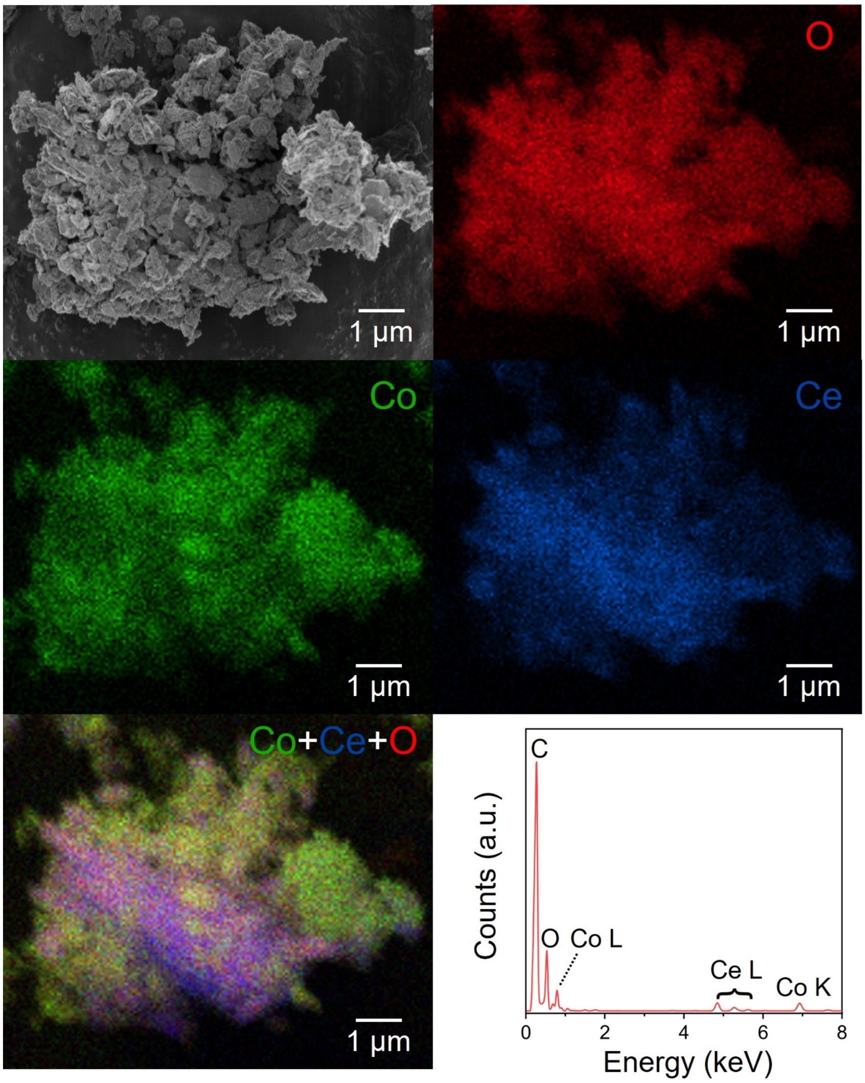

Fig. S2 SEM image of Co_3Ce support together with EDX spectrum and maps of O, Co and Ce.

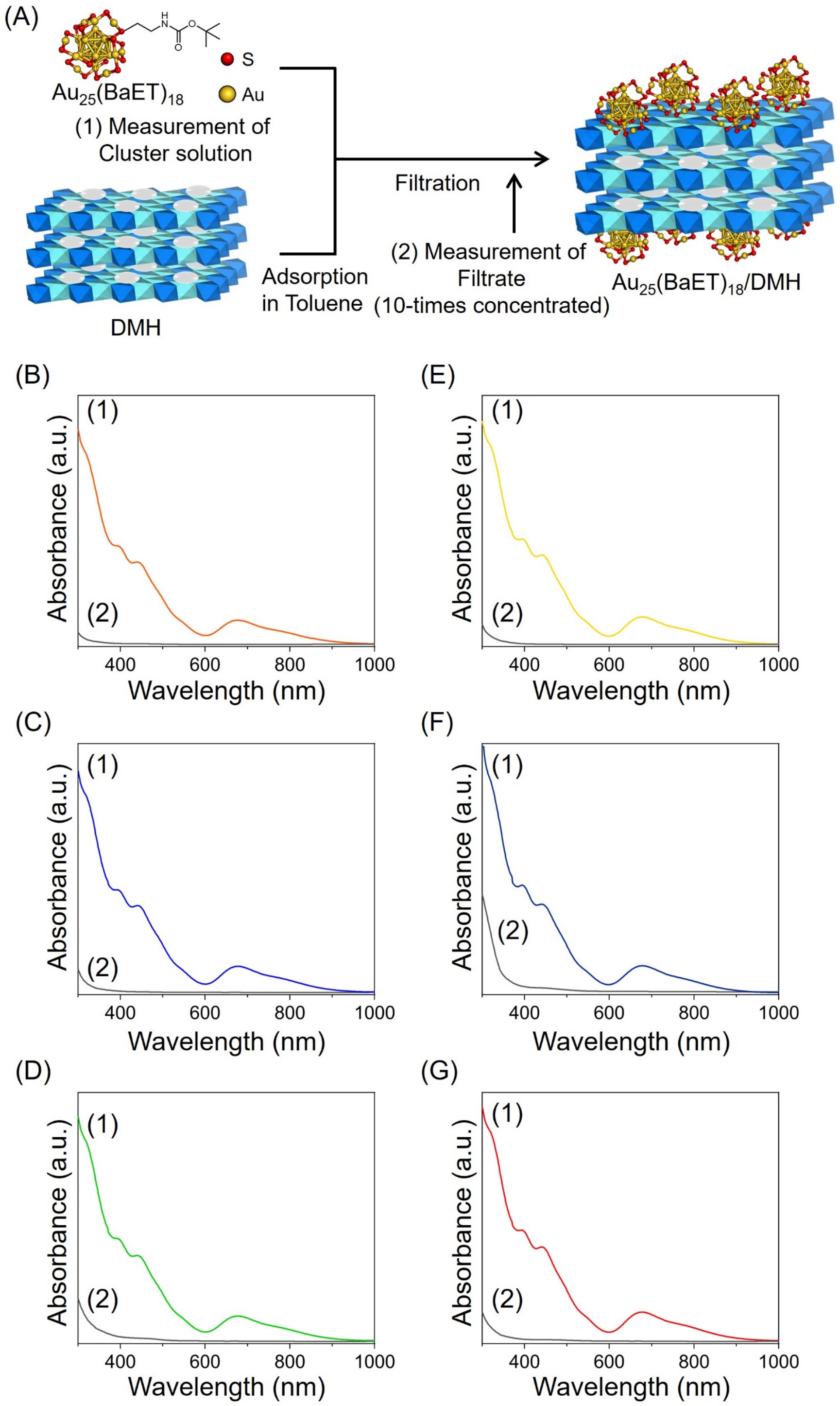

Fig. S3 (A) Schematic illustration of adsorption of $Au_{25}(BaET)_{18}^-$ onto various DMH supports. UV-vis absorption spectra of (1) cluster solution and (2) the filtrate after adsorption onto (B) Mg_3Al, (C) Ni_3Al, (D) Co_3Al, (E) Mg_3Ce, (F) Ni_3Ce and (G) Co_3Ce.

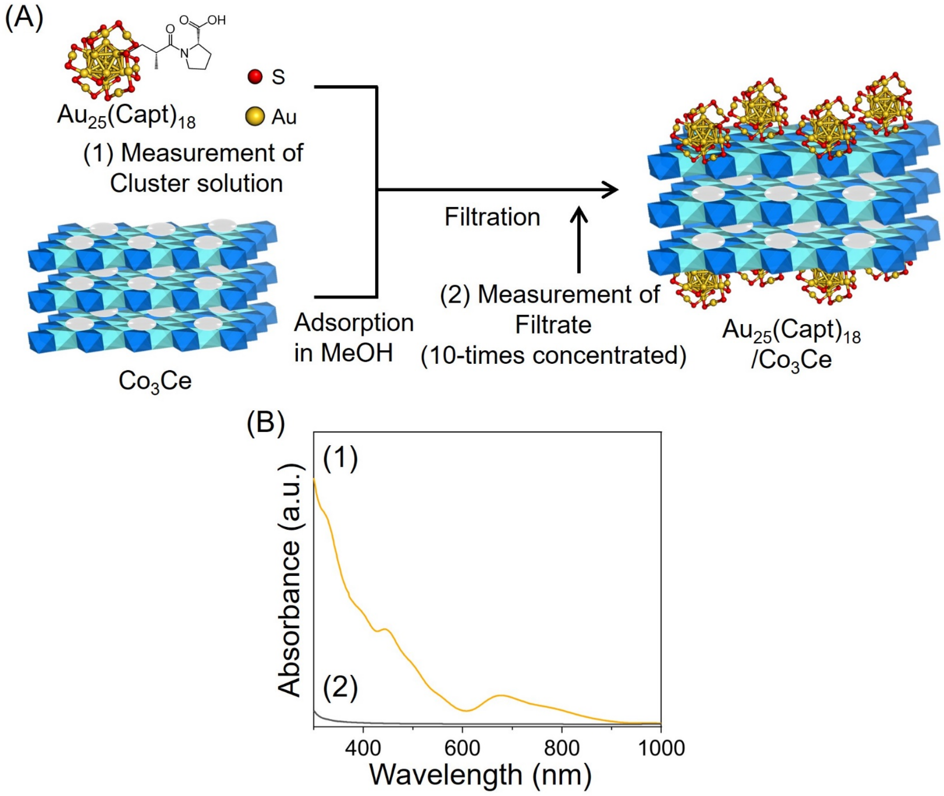

Fig. S4 (A) Schematic illustration of adsorption of $Au_{25}(Capt)_{18}^-$ onto Co_3Ce. (B) UV-vis absorption spectra of (1) cluster solution and (2) the filtrate after adsorption onto Co_3Ce.

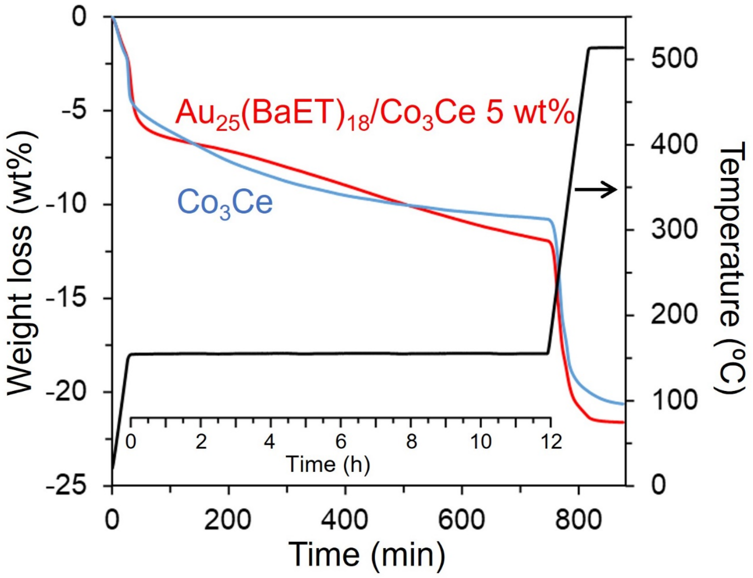

Fig. S5 TG analyses of raw Co_3Ce and $Au_{25}(BaET)_{18}/Co_3Ce$. The heating rate was fixed to 5 °C/min and kept at 150 °C for 12 h.

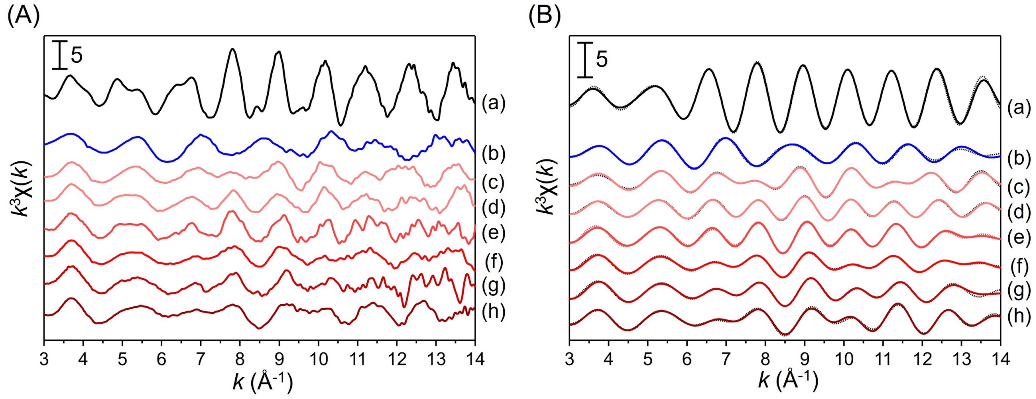

Fig. S6 (A) EXAFS oscillations and (B) fitting curves of EXAFS in k-space over the *r* range of 1.4–3.1 Å of (a) Au foil, (b) Au$_{25}$(BaET)$_{18}$/Co$_3$Ce, and Au$_{25}$(BaET)$_{18}$/Co$_3$Ce-150-*t* with *t* = (c) 2, (d) 4, (e) 8, (f) 12, (g) 20, and (h) 30, respectively.

Table S2 Structural parameters of Au$_{25}$(BaET)/Co$_3$Ce-150-*t* obtained by curve-fitting analysis of EXAFS in Fig. S6A

sample	bond	*CN*[a]	*r* (Å)[b]	σ (Å^2)[c]	R (%)[d]
Au foil	Au–Au	12.0(3)	2.85(2)	0.0085(2)	9.3
Au$_{25}$(BaET)$_{18}$/Co$_3$Ce	Au–S	1.8(2)	2.33(4)	0.0066(10)	14.5
	Au–Au	0.7(2)	2.72(3)	0.0058(20)	
Au$_{25}$(BaET)$_{18}$/Co$_3$Ce-150-2	Au–S	0.7(1)	2.30(4)	0.0022(17)	12.2
	Au–Au	2.8(3)	2.87(4)	0.0079(9)	
Au$_{25}$(BaET)$_{18}$/Co$_3$Ce-150-4	Au–S	0.8(2)	2.27(7)	0.0114(33)	9.6
	Au–Au	4.7(3)	2.84(4)	0.0096(6)	
Au$_{25}$(BaET)$_{18}$/Co$_3$Ce-150-8	Au–S	0.4(2)	2.29(6)	0.0041(31)	14.9
	Au–O	1.2(2)	2.02(5)	0.0029(20)	
	Au–Au	5.8(4)	2.81(4)	0.0108(6)	
Au$_{25}$(BaET)$_{18}$/Co$_3$Ce-150-12	Au–O	1.2(2)	2.02(5)	0.0045(22)	10.9
	Au–Au	4.7(4)	2.83(5)	0.0128(12)	
Au$_{25}$(BaET)$_{18}$/Co$_3$Ce-150-20	Au–O	1.7(3)	2.01(5)	0.0077(21)	14.9
	Au–Au	3.1(2)	2.78(3)	0.0061(5)	
	Au–Au	1.1(2)	2.91(4)	0.0038(12)	
Au$_{25}$(BaET)$_{18}$/Co$_3$Ce-150-30	Au–O	1.1(2)	2.00(4)	0.0026(25)	14.7
	Au–Au	1.4(2)	2.80(4)	0.0044(9)	
	Au–Au	3.2(6)	2.93(8)	0.0135(34)	

[a]Coordination number. [b]Bond length. [c]Debye-Waller factor. [d]$R = (\sum(k^3\chi^{\mathrm{data}}(k) - k^3\chi^{\mathrm{fit}}(k))^2)^{1/2}/(\sum(k^3\chi^{\mathrm{data}}(k))^2)^{1/2}$. Figures in parentheses show errors.

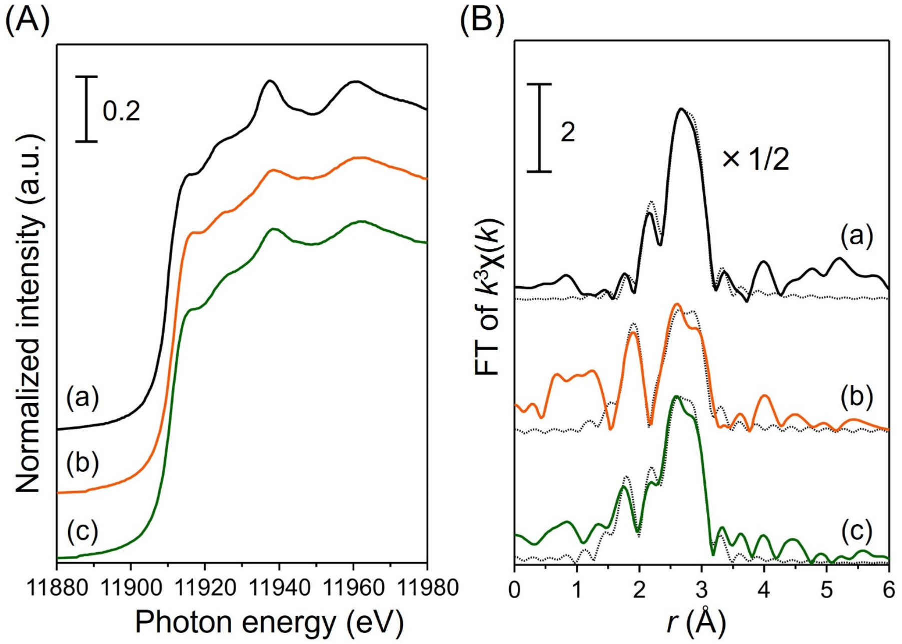

Fig. S7 (A) XANES spectra and (B) Fourier transform of EXAFS of (a) Au foil, (b) $Au_{25}(BaET)_{18}/Co_3Ce$-150-12 aged *in vacuo.* and (c) $Au_{25}(BaET)_{18}/CeO_2$-150-12 aged in air. Solid line: raw data, dashed line: fitting data.

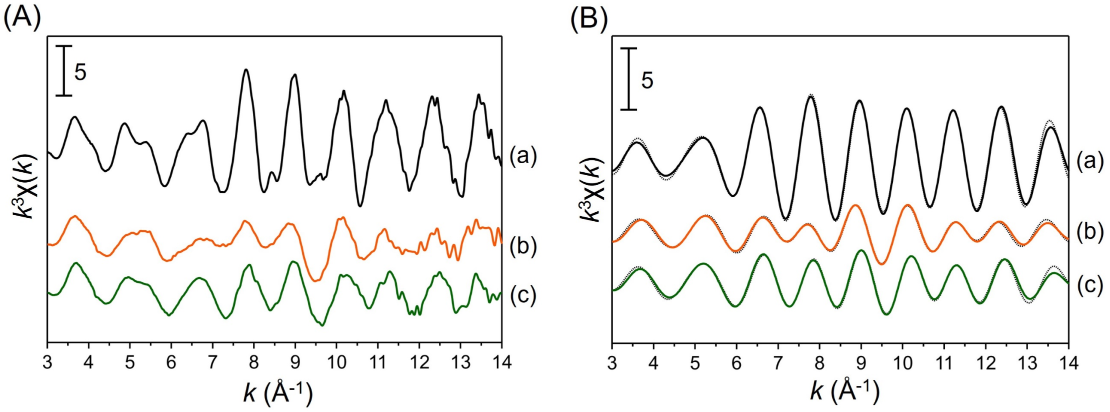

Fig. S8 (A) EXAFS oscillations and (B) fitting curves of EXAFS in k-space over the r range of 1.4–3.1 Å of (a) Au foil, (b) $Au_{25}(BaET)_{18}/Co_3Ce$-150-12 aged *in vacuo.* and (c) $Au_{25}(BaET)_{18}/CeO_2$-150-12 aged in air. Solid line: raw data, dashed line: fitting data.

Table S3 Structural parameters of each sample obtained by curve-fitting analysis of EXAFS in Fig. S8A

sample	bond	*CN*[c]	*r* (Å)[d]	σ (Å^2)[e]	R (%)[f]
$Au_{25}(BaET)_{18}/Co_3Ce$-150-12[a]	Au–S	0.9(2)	2.34(5)	0.0048(16)	13.2
	Au–Au	5.3(3)	2.85(4)	0.0100(6)	
$Au_{25}(BaET)_{18}/CeO_2$-150-12[b]	Au–S	0.5(2)	2.24(6)	0.0050(29)	13.8
	Au–Au	6.4(3)	2.83(3)	0.0096(5)	

[a] Aged *in vacuo*. [b] Aged in air. [c] Coordination number. [d] Bond length. [e] Debye-Waller factor. [f] $R=(\sum(k^3\chi^{data}(k)- k^3\chi^{fit}(k))^2)^{1/2}/(\sum(k^3\chi^{data}(k))^2)^{1/2}$. Figures in parentheses show errors.

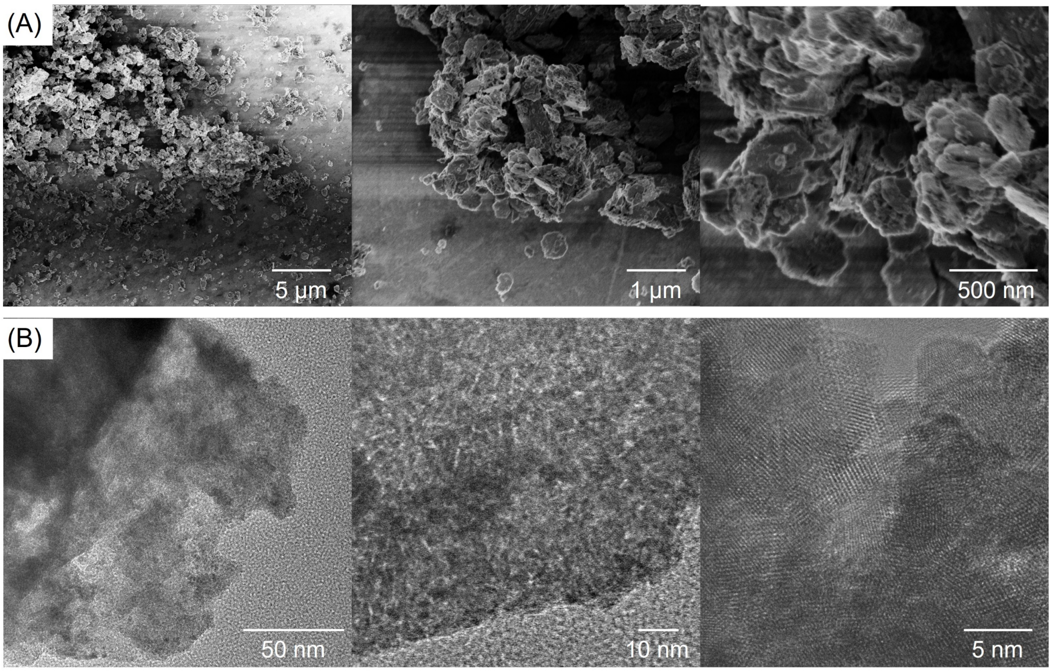

Fig. S9 (A) SEM and (B) ACTEM images of Au_{25}/Co_3Ce.

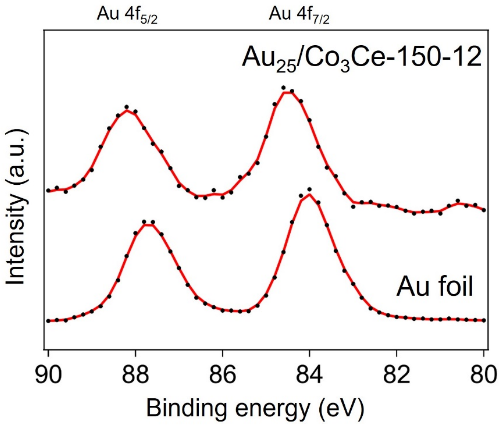

Fig. S10 Au 4f XPS spectra of Au foil and Au_{25}/Co_3Ce.

Table S4 Summary of previous studies on catalytic oxidation of benzyl alcohol

sample	solvent	temp. (ºC)	mol%	time	conversion (%)	selectivity (%)	TON	TOF (h^{-1})	ref.
Au_{25}/Co_3Ce	water	30	0.1	2 h	>99	>99 (acid)	997	1097	This work
Au/Mesoporous C[a]	water	25	0.063	24 h	>99	>99 (acid)	1600	478 (surface)	S5
Au/Mesoporous C[b]	water	60	0.056	5 h	>99	>99 (acid)	1800	1638 (surface)	S5
Au/Mesoporous C[c]	water	60	0.063	12 h	>99	>99 (acid)	1600	384	S6
Au:PVP[d]	water	27	2.0	6 h	85	100 (acid)	43	13.5	S7
Au/CeO_2_N[e]	water	40	2.36	2 h	98	100 (acid)	41	—	S8
Au_{25}/HPCS[f]	water	30	2.20	6 h	98	70 (acid)	45	—	S9
Au_{25}/HPCS[f]	water	30	2.20	10 min	77	47 (acid)	35	210	S9
Au_{144}/HPC[f]	water	30	2.20	30 min	~82	—	—	~200 (surface)	S10
Au_{38}/Ni_3Al-LDH[g]	toluene	100	0.20	10 min	62.8	>99 (aldehyde)	—	1884	S11
Au/Cr4-HT[h]	toluene	100	0.079	30 min	72	>99 (aldehyde)	1830	1830	S12
Au/Cr4-HT[i]	toluene	100	0.05	30 min	76	>99 (aldehyde)	3040	3040	S12
Au-SA/CeO_2-NR[j]	toluene	100	0.2	30 h	89	94 (aldehyde)	470	193	S13
Au-100CeO_2@SBA-15[k]	toluene	90	0.4	10 min	18	>99 (aldehyde)	—	270	S14
Au/MgO[i]	toluene	110	0.5	30 min	98	92 (aldehyde)	—	752	S15

[a]KOH 400 mol%, 800 rpm, O_2, surface atom/total atom = 0.40. [b]KOH 400 mol%, 800 rpm, O_2, surface atom/total atom = 0.17. [c]KOH 400 mol%, TOF is calculated at 15 min. [d]K_2CO_3 300 mol%, air. [e]NaOH 100 mol%, 800 rpm, O_2. [f]K_2CO_3 63 mol%, O_2. [g]Base free, air. [h]Base free, Au 0.31 wt%, O_2. [i]Base free, Au 0.13 wt%, O_2. [j]Base free, O_2, TOF is calculated at 20 min. [k]Base free, O_2. [l]Base free, O_2.

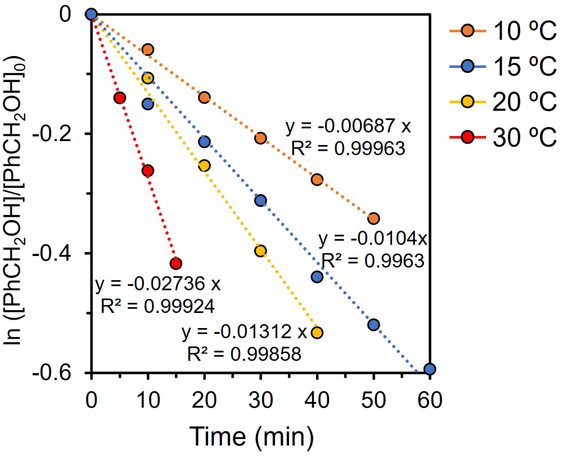

Fig. S11 The reaction kinetics as a function of temperature. Reaction conditions: benzyl alcohol 761 μmol (0.1 mol%), Au$_{25}$/Co$_3$Ce 15 mg, KOH 300 mol%, water 15 mL, O$_2$ 1 atm (balloon), 10–30 °C.

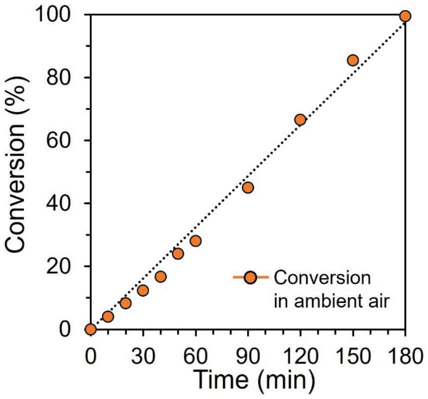

Fig. S12 Time course of the conversion for oxidation of PhCH$_2$OH catalyzed by Au$_{25}$/Co$_3$Ce. Reaction conditions: Au 0.1 mol%, KOH 300 mol%, water, 30 °C, ambient air.

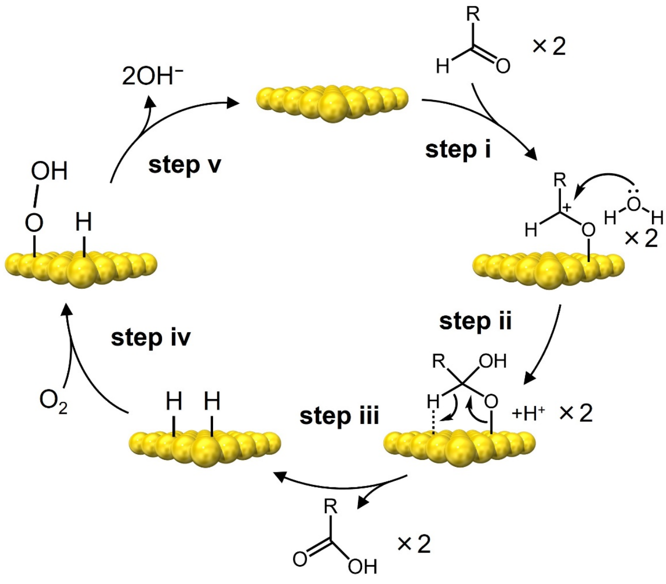

Scheme S1 Possible oxidation pathway of PhCHO to PhCO$_2$H on Au$_{25}$/Co$_3$Ce in water.

3. References

S1. S. Wang, S. Yin, G. Chen, L. Li and H. Zhang, *Catal. Sci. Technol.*, 2016, **6**, 4090–4104.

S2. M. A. Tofanelli, K. Salorinne, T. W. Ni, S. Malola, B. Newell, B. Phillips, H. Häkkinen and C. J. Ackerson, *Chem. Sci.*, 2016, **7**, 1882–1890.

S3. S. Kumar and R. Jin, *Nanoscale*, 2012, **4**, 4222–4227.

S4. H. Asakura, S. Yamazoe, T. Misumi, A. Fujita, T. Tsukuda and T. Tanaka, *Radiat. Phys. Chem.* , 2020, **175**, 108270.

S5. S. Wang, J. Wang, Q. Zhao, D. Li, J.-Q. Wang, M. Cho, H. Cho, O. Terasaki, S. Chen and Y. Wan, *ACS Catal.*, 2015, **5**, 797–802.

S6. Wang, S.*, et al.* Aggregation-Free Gold Nanoparticles in Ordered Mesoporous Carbons: Toward Highly Active and Stable Heterogeneous Catalysts. *J. Am. Chem. Soc.* **135**, 11849–11860 (2013).

S7. S. Wang, Q. Zhao, H. Wei, J.-Q. Wang, M. Cho, H. S. Cho, O. Terasaki and Y. Wan, *J. Am. Chem. Soc.*, 2013, **135**, 11849–11860.

S8. L. Wolski, G. Nowaczyk, S. Jurga and M. Ziolek, *Catalysts*, 2021, **11**, 641.

S9. T. Yoskamtorn, S. Yamazoe, R. Takahata, J.-i. Nishigaki, A. Thivasasith, J. Limtrakul and T. Tsukuda, *ACS Catal.*, 2014, **4**, 3696–3700.

S10. S. Yamazoe, T. Yoskamtorn, S. Takano, S. Yadnum, J. Limtrakul and T. Tsukuda, *Chem. Rec.*, 2016, **16**, 2338–2348.

S11. Y. Xu, J. Li, J. Zhou, Y. Liu, Z. Wei and H. Zhang, *J. Catal.*, 2020, **389**, 409–420.

S12. P. Liu, V. Degirmenci and E. J. M. Hensen, *J. Catal.*, 2014, **313**, 80–91.

S13. L. Lei, H. Liu, Z. Wu, Z. Qin, G. Wang, J. Ma, L. Luo, W. Fan and J. Wang, *ACS Appl. Nano Mater.*, 2019, **2**, 5214–5223.

S14. T. Wang, X. Yuan, S. Li, L. Zeng and J. Gong, *Nanoscale*, 2015, **7**, 7593–7602.

S15. Z. Wang, C. Xu and H. Wang, *Catal. Lett.*, 2014, **144**, 1919–1929.